DOI: 10.13009/EUCASS2019-252

Wall-Modeled Large Eddy Simulation for Predicting Wall Heat Flux in a Rocket Combustion Chamber

Daiki Muto⋆*, Yu Daimon*⋆⋆*, Taro Shimizu*⋆*, and Hideyo Negishi*⋆⋆*
⋆*Japan Aerospace Exploration Agency*
3-1-1 Yoshinodai, Chuo-ku, Sagamihara, Kanagawa, Japan, muto.daiki@jaxa.jp
⋆⋆*Japan Aerospace Exploration Agency*
2-1-1 Sengen, Tsukuba, Ibaraki, Japan, daimon.yu@jaxa.jp
⋆⋆*Japan Aerospace Exploration Agency*
3-1-1 Yoshinodai, Chuo-ku, Sagamihara, Kanagawa, Japan, shimizu.taro@jaxa.jp
⋆⋆*Japan Aerospace Exploration Agency*
2-1-1 Sengen, Tsukuba, Ibaraki, Japan, negishi.hideyo@jaxa.jp

Abstract

The present study performs wall-modeled large eddy simulation (WMLES) of a hydrogen/oxygen rocket combustion chamber for accurate prediction of wall heat flux. A wall model developed for reacting flows is coupled with LES solving the flamelet progress-variable approach. Results demonstrate that WMLES well predicts the wall heat flux overall even with a coarse near-wall grid and at an acceptable computational cost for solving the wall model. However, the peak of wall heat flux is underestimated, indicating that grid sensitivity study is needed.

1. Introduction

Prior evaluation of engine performance and assessing potential risks is crucial in designing liquid rocket combustion chambers. One of the risks identified as a critical event is wall damage or melting caused by an excessive heat load on the chamber wall. Near the wall, a drastic temperature gradient is developed between free-stream burnt gas and the cooled wall, resulting in the chamber wall is exposed to a high heat flux that can locally reach 100 MW/m^2, and such a high heat flux could lead to serious wall damages. Since reusable rocket engines have come into focus by the space community, the importance of an accurate prediction of wall heat flux will be increased for estimating chamber lifetimes. Also, the field of industrial combustion chambers, such as those in gas turbines and automotive engines, requires accurate estimation of wall heat loss to improve engine performance in terms of thermal efficiency.

Large eddy simulation (LES) is a powerful approach for simulating unsteady and complex turbulent combustion fields, and a number of LES studies has demonstrated its validity for simulating combustion chambers. However, a major challenge of LES is a huge computational cost for resolving turbulent boundary layer. A near-wall computational grid resolving the viscous length scale of O (1 μm) drastically increases the number of grid points and decreases the time step. Because of this constraint, LES of combustion chambers has often used a computational grid that is too coarse to resolve the near-wall flows. If near-wall flows are not properly resolved, wall shear stress and heat flux are of course not well obtained.

To overcome this issue, a wall-modeled LES (WMLES) is expected to be promising approach.[1] The idea behind WMLES is resolving the outer layer while modeling the inner layer, as inner layer models are used to estimate wall shear stress and heat flux. The validity of WMLES has been recently demonstrated regarding aerodynamic problems,[2,3] but its application to reacting flows is still limited.[4]

WMLES generally models the inner layer by solving coupled ordinary differential equations (ODEs) for velocity and temperature derived with the equilibrium-stress boundary-layer approximation.[5] For reacting flows, however, the existing inner layer models essentially does not work because they assume non-reacting single component flows. Near the chamber wall, chemical reactions occur due to the heat loss from the burnt gas to the cooled wall, and the chemical composition gradually changes within the boundary layer. Changes in temperature and chemical composition result in a considerable variation in mixture properties. Several studies have shown that these near-wall chemical and thermal effects have a non-negligible impact on the wall heat flux calculation.[6,7] Therefore, applying WMLES for reacting flows requires an inner layer model that considers these near-wall physics. Muto et al. recently proposed a

DOI: 10.13009/EUCASS2019-252

wall model for reacting flows that includes variable property and chemical effects.[8] In this wall model, based on the boundary-layer approximation with a chemical equilibrium assumption, two coupled ODEs of velocity and temperature are solved. A pre-tabulated database generated from a chemical equilibrium calculation is used to estimate the chemical contributions. This wall model, referred as the equilibrium wall model, accurately reproduces the inner layer of hydrogen/oxygen reacting flows in their a priori study; the wall model was tested without coupling with LES.

The objective of this study is to assess the validity of WMLES for predicting wall heat flux in reacting flows using the equilibrium wall model. We preliminary performs WMLES of a hydrogen/oxygen rocket combustion chamber, and the wall heat flux is compared with the existing LES and measured results. As a combustion model of LES, the flamelet progress-variable (FPV) approach is used.

2. Numerics

2.1 Numerical method for LES

The present LES is performed by using JAXA's in-house CFD solver LS-FLOW, which is an arbitrary polyhedral unstructured compressible flow solver[9] that solves the three-dimensional compressible Navier-Stoke equations for conserved variables of mass, momentum, and total energy. The equations are closed with the ideal gas equation of state. The Green-Gauss method is used as a gradient calculation for reconstruction. The method by Venkatakrishnan[10] is used as a gradient limiting function. The convective terms are evaluated using SLAU2.[11] The method by Marvriplis[12] is used for viscous term calculations. For time integration, the LU-SGS implicit method is used with three sub-iterations. The Wall-Adapting Local Eddy-viscosity (WALE) model[13] is used to calculate the SGS eddy viscosity.

For turbulent combustion modeling, the flamelet progress-variable approach[14] is applied, which solves transport equations for mixture fraction and progress variable. The mixture fraction variance is determined from an algebraic expression. The turbulent Prandtl and Schmidt numbers are set to 0.9. The progress variable is taken here as the mass fraction of H_2O. The species mass fractions are tabulated in terms of the mixture fraction, mixture fraction variance, and progress variable. A reaction mechanism by Petersen and Hanson[15] is used in generating the flamelet table.

2.2 Equilibrium wall model

LES is coupled with the equilibrium wall model.[8] With the boundary-layer approximation and the chemical equilibrium assumption, the boundary layer equations for velocity and temperature are obtained as follows:

$$\frac{d}{dy}\left[(\mu+\mu_t)\frac{dU_{\parallel}}{dy}\right]=0, \tag{1}$$

$$\frac{d}{dy}\left[\left(\lambda+\frac{c_p\mu_t}{Pr_t}+\frac{\mu}{Sc}\sum_{k=1}^{N}h_k\left.\frac{dY_k}{dT}\right|_{\text{eq.}}+\frac{\mu_t}{Sc_t}\sum_{k=1}^{N}\Delta h^o_{f,k}\left.\frac{dY_k}{dT}\right|_{\text{eq.}}\right)\frac{dT}{dy}\right]+\frac{d}{dy}\left[(\mu+\mu_t)U_{\parallel}\frac{dU_{\parallel}}{dy}\right]=0. \tag{2}$$

where $U_{\parallel}$ is the wall parallel velocity, μ is the viscosity, T is the temperature, λ is the thermal conductivity, c_p is the specific heat at constant pressure. h_k, Y_k, and $\Delta h^o_{f,k}$ are the enthalpy, mass fraction, and the chemical enthalpy of formation of species k, respectively. μ_t, Pr_t, and Sc_t are the eddy viscosity and the turbulent Prandtl and Schmidt number, respectively. Here, no radiation, no Dufour and Soret effects, and equal diffusivities for all species are assumed.

Even though chemical equilibrium is assumed, these equations can describe the velocity and temperature in the inner layer of reacting flows. This is explained that the chemical time scale is sufficiently smaller than the flow time scale in the inner layer, so the inner layer flow can always be assumed to reach chemical equilibrium.[8]

The inner-layer eddy viscosity is modeled by using the mixing length model:[16]

$$\mu_t=\kappa\rho\sqrt{\frac{\tau_w}{\rho}}y[1-\exp(-y^\star/A^+)]^2, \tag{3}$$

where τ_w is the wall shear stress, and κ=0.41 and $A^+=17$ are model constants. Here, instead of the classical wall units of $y^+=\rho_w u_\tau y/\mu_w$ and $u_\tau=\sqrt{\tau_w/\rho_w}$, $y^*=\rho u^*_\tau y/\mu$ and $u^*_\tau=\sqrt{\tau_w/\rho}$ known as the semi-local properties are used. It has been found that the semi-local properties are appropriate for the scaling of the near-wall flows with significant heat transfer.[17,18]

The coupled ODEs of Eqs. 1 and 2 with the mixing length model of Eq. 3 are numerically solved by using a one-dimensional finite volume method. A table look-up procedure is used to estimate the chemical factors

DOI: 10.13009/EUCASS2019-252

of $\sum_{k=1}^{N} h_k \left(dY_k/dT\right)_{\text{eq.}}$ and $\sum_{k=1}^{N} \Delta h^o_{f,k} \left(dY_k/dT\right)_{\text{eq.}}$ in Eq. 2, and the thermodynamic and transport properties of the mixture. These values at a chemical equilibrium corresponding to given temperature, pressure, and initial chemical composition are pre-tabulated. The look-up table is generated from the equilibrium calculation using CEA.[19] Here, $Sc = Pr$ is applied with assuming the Lewis number is unity, where $Pr = \mu c_p/\lambda$ is the Prandtl number. A model constant of Pr_t and Sc_t are set to a value of 0.9.

To couple the wall model with LES, the transport equations for mixture fraction and progress variable need to be closed since LES does not solve the near-wall flow. In the present implementation, a zero-flux condition at the wall is assumed for both equations. While this holds for the mixture fraction because its transport equation does not include a source term, the transport equation for the progress variable does have one. Thus, the zero-flux condition for the progress variable is a first approximation; it is assumed to have only a minor influence on the progress of chemical reactions in freestream.

3. Flow configuration and computational grid

The present WMLES is applied to a single-element oxygen/hydrogen combustor,[20,21] which consists of a coaxial element and a chamber with a diameter of 38.1 mm. The gaseous oxidizer and fuel are injected from the center and annular injectors of the coaxial element. The exit diameter of the central oxidizer jet is 5.26 mm, and the exit inner and outer diameters of the annular fuel jet are 6.30 and 7.49 mm, respectively. The composition of the oxidizer is $Y_{O_2} = 0.945$ and $Y_{H_2O} = 0.055$, and that of the fuel is $Y_{H_2} = 0.402$ and $Y_{H_2O} = 0.598$. The mass flow rates of oxidizer and fuel are 0.0904 kg/s and 0.0331 kg/s, and the inlet temperatures are 711 K and 800 K, respectively. The Reynolds numbers based on the bulk exit velocities and hydraulic diameters are 6.04×10^5 and 1.69×10^5 for the oxidizer and fuel jet, respectively. The operating pressure is 5.2 MPa.

The mass flow rates and temperature are specified at the inlets of the LES domain. The turbulence is generated behind the edge of the coaxial injector using the method by Bogey et al.[22] The measured wall temperature profile is specified along the chamber wall.[20] The temperature of 755 K is applied at the face of the chamber and the post tip. The supersonic outflow condition is applied at the outlet.

The number of the LES grids is approximately 61 million. The LES domain starts 2.5 mm upstream of the face of the chamber, and the grids are clustered near the injector exit and the wall. Note that as the use of the wall model, the near-wall grid needs to be able to resolve energetic eddies in the outer layer. The boundary layer gradually develops throughout the chamber and reaches about 2 mm thick at x =200 mm. At x =200 mm, the grid spacing near the edge of the boundary layer is 0.2 mm both streamwise and circumferential directions. The wall-normal grid spacing is 0.2 mm at the edge of the boundary layer and smoothly refined towards the wall where the spacing is 0.04 mm. The boundary layer is resolved over approximately 25 points in the direction normal to the wall at x =200 mm.

The wall-model grid is embedded in the LES grid, which is 0.2 mm thick and has 41 grid points. At the top boundary of the wall model, a set of instantaneous LES solutions of wall-parallel velocity, temperature, pressure, and chemical compositions is applied. Non-slip and iso-thermal boundary conditions are applied at the bottom boundary. After the wall-model is solved, the obtained wall shear stress and wall heat flux are fed back to the LES as wall boundary conditions.

4. Results

Figure 1 shows the instantaneous fields of temperature, giving the overall flow features. Wrinkled diffusion flames are generated between the oxidizer and fuel flows, and are held behind the oxidizer posts. The low-temperature region behind the injector exit corresponds to pure oxidizer. Recirculation develops near the corner, which entrains the surrounding gas towards the wall. A thermal boundary layer gradually develops at the wall according to the wall heat loss.

Figure 2 compares the circumferentially-averaged mean wall heat flux along the chamber wall with the results of experiment[20] and existing LES that resolve the wall. The result demonstrates that the present WMLES accurately predicts wall heat flux at the downstream region from x = 150 mm. The near-injector rise in the wall heat flux is also well captured. Note that the location of the first grid point off the wall is approximately 20 in wall units at x = 200 mm. Even with such a coarse near-wall grid, the wall heat flux is well predicted overall owing to the wall model. The additional cost for solving the wall model is approximately 10%. It is estimated that the computational cost is reduced by two to three orders of magnitude compared with that of the conventional wall-resolved LES for two reasons: reducing the number of grid points and increasing the time step.

However, the underprediction of the peak heat flux is observed between x = 50 mm and 150 mm. This is likely because that the present computational grid is designed to resolve the eddies in developed boundary layer; the

DOI: 10.13009/EUCASS2019-252

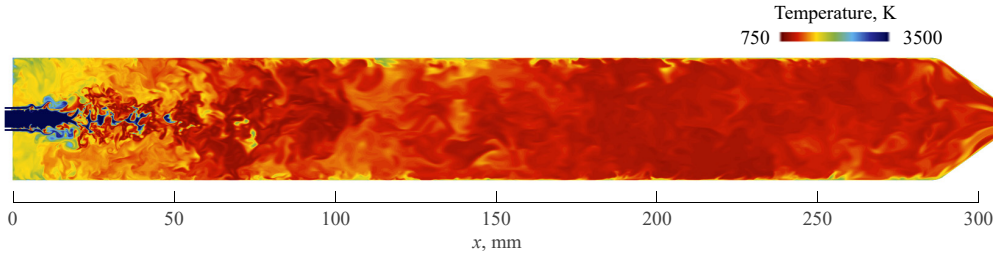

Figure 1: Instantaneous temperature field.

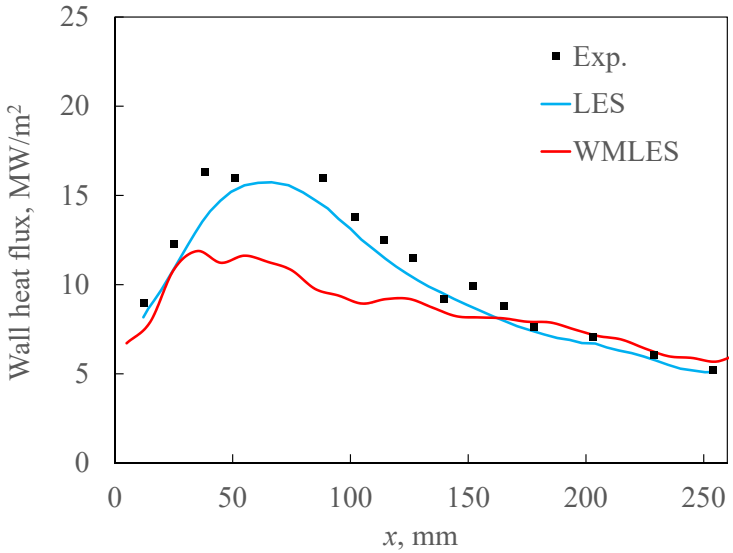

Figure 2: Averaged wall heat flux profiles of WMLES compared with the results of LES and experiment[20]

grid resolution could be coarse at the region where the boundary layer is thin. It is needed to investigate whether the near-wall grid resolution is sufficient to resolve energetic eddies in the outer layer around this region.

5. Conclusions

An application of a wall model for LES of reacting flows was presented for predicting the wall heat flux in combustion chambers. A wall model including thermal and chemical effects was coupled with LES solving the flamelet progress-variable approach and preliminary tested in a hydrogen/oxygen rocket combustion chamber. The results demonstrated that WMLES predicted the measured wall heat flux where the near-injector and downstream regions accurately, even with a coarse near-wall grid. The additional cost for solving the wall model is acceptable. However, the underestimation of the wall heat flux was observed around the region where the boundary layer is thin, indicating the need of grid sensitivity study.

The present work only deals with a hydrogen/oxygen combustion, and an applicability of the present WMLES approach for hydrocarbon reacting flows is a subject for future study.

Acknowledgments

The present simulation was performed on JAXA Supercomputer System generation 2 (JSS2).

References

[1] Larsson, J., Kawai, S., Bodart, J., and Bermejo-Moreno, I. 2016. Large eddy simulation with modeled wall-stress: recent progress and future directions. *Mechanical Engineering Reviews*, 3, 1 15–00418.

DOI: 10.13009/EUCASS2019-252

[2] Bodart, J., and Larsson, D. J. 2011. Wall-modeled large eddy simulation in complex geometries with application to high-lift devices. *Center for Turbulence Research Annual Research Briefs*, 37–48.

[3] Fukushima, Y., and Kawai, S. 2018. Wall-modeled large-eddy simulation of transonic airfoil buffet at high Reynolds number. *AIAA Journal*, 56, 6.

[4] Larsson, J., Laurence, S., Bermejo-Moreno, I., Bodart, J., Karl, S., and Vicquelin, R. 2015. Incipient thermal choking and stable shock-train formation in the heat-release region of a scramjet combustor. Part II: Large eddy simulations. *Combustion and Flame*, 162, 4, 907–920.

[5] Kawai, S., and Larsson, J. 2012. Wall-modeling in large eddy simulation: Length scales, grid resolution, and accuracy. *Physics of Fluids*, 24, 015105.

[6] Betti, B., Bianchi, D., Nasuti, F., and Martelli, E. 2016. Chemical reaction effects on heat loads of CH4/O2 and H2/O2 rockets. *AIAA Journal*, 54, 5, 1693–1703.

[7] Kitano, T., Iida, H., and Kurose, R. 2017. Effect of chemical reactions of H2/O2 combustion gas on wall heat flux in a turbulent channel flow. *Journal of Heat Transfer*, 139.

[8] Muto, D., Daimon, Y., Shimizu, T., and Negishi, H. An equilibrium wall model for reacting turbulent flows with heat transfer. *International Journal of Heat and Mass Transfer* (accepted on May 2019).

[9] Kitamura, K., Fujimoto, K., Shima, E., Kuzuu, K., and Wang, Z. 2011. Validation of arbitrary unstructured CFD code for aerodynamic analyses. *Transactions of the Japan Society for Aeronautical and Space Sciences*, 53, 182, 311–319.

[10] Venkatakrishnan, V. 1995. Convergence to steady state solutions of the Euler equations on unstructured grids with limiters. *Journal of Computational Physics*, 118, 120–130.

[11] Kitamura, K., and Shima, E. 2013. Towards shock-stable and accurate hypersonic heating computations: A new pressure flux for AUSM-family schemes. *Journal of Computational Physics*, 245, 62–83.

[12] Mavriplis, D. J. 2008. Unstructured-mesh discretizations and solvers for computational aerodynamics. *AIAA Journal*, 46, 6, 1281–1298.

[13] Nicoud, F., and Ducros, F. 1999. Subgrid-scale stress modelling based on the square of the velocity gradient tensor. *Flow, Turbulence and Combustion*, 62, 183–200.

[14] Pierce, C. D., and Moin, P. 2004. Progress-variable approach for large-eddy simulation of non-premixed turbulent combustion. *Journal of Fluid Mechanics*, 504, 73–97.

[15] Petersen, E. L., and Hanson, R. K. 1999. Reduced kinetics mechanisms for ram accelerator combustion. *Journal of Propulsion and Power*, 15, 4, 591–600.

[16] Yang, X. I., and Lv, Y. 2018. A semi-locally scaled eddy viscosity formulation for LES wall models and flows at high speeds. *Theoretical and Computational Fluid Dynamics*, 32, 617–627.

[17] Trettel, A., and Larsson, J. 2016. Mean velocity scaling for compressible wall turbulence with heat transfer. *Physics of Fluids*, 28, 026102.

[18] Huang, P. G., Coleman, G. N., and Bradshaw, P. 1995. Compressible turbulent channel flows: DNS results and modeling. *Journal of Fluid Mechanics*, 305, 185–218.

[19] Gordon, S., and McBride, B. J. 1994. Computer Program for Calculation of Complex Chemical Equilibrium Compositions and Applications.

[20] Tucker, P., Menon, S., Merkle, C., Oefelein, J., and Yang, V. 2008. Validation of high-fidelity CFD simulations for rocket injector design. In: *44th AIAA/ASME/SAE/ASEE Joint Propulsion Conference & Exhibit*, AIAA 2008-5226.

[21] Pal, S., Marshall, W., Woodward, R., and Santoro, R., 2006. Wall heat flux measurements for a uni-element GO2/CH2 shear coaxial injector. In: *3rd International Workshop on Rocket Combustion Modeling*.

[22] Bogey, C., Bailly, C., and Juve, D. 2003. Noise investigation of a high subsonic, moderate-Reynolds-number jet using compressible Large eddy simulation. *Theoretical and Computational Fluid Dynamics*, 16, 273–297.